Loss of Raptor induces Sertoli cells into an undifferentiated state in mice

Authors: Xie, Minyu, Hu, Xiao, Li, Lei, Xiong, Zhi, Zhang, Hanbin, et al.

Source: Biology of Reproduction, 107(4) : 1125-1138

Published By: Society for the Study of Reproduction

URL: https://doi.org/10.1093/biolre/ioac104

Biology of Reproduction, 2022, **107(4)**, 1125–1138
https://doi.org/10.1093/biolre/ioac104
Advance access publication date 19 May 2022
Research Article

Loss of *Raptor* induces Sertoli cells into an undifferentiated state in mice

Minyu Xie[1,2,†], Xiao Hu[3,†], Lei Li[1,†], Zhi Xiong[4], Hanbin Zhang[2], Yuge Zhuang[2], Zicong Huang[2], Jinsheng Liu[2], Jingyao Lian[5], Chuyu Huang[6], Qiang Xie[7], Xiangjin Kang[5,*], Yong Fan[5,*], Xiaochun Bai[8,*] and Zhenguo Chen[2,*]

[1]Department of Obstetrics and Gynecology, Center for Reproductive Medicine; Department of Fetal Medicine and Prenatal Diagnosis, BioResource Research Center, Guangdong Provincial Key Laboratory of Major Obstetric Diseases, The Third Affiliated Hospital of Guangzhou Medical University, Guangzhou Guangdong, China
[2]Guangdong Provincial Key Laboratory of Construction and Detection in Tissue Engineering, Department of Cell Biology, School of Basic Medical Sciences, Southern Medical University, Guangzhou, Guangdong, China
[3]Department of Plastic and Burn Surgery, Guangzhou Red Cross Hospital, Jinan University Faculty of Medical Science, Guangzhou, Guangdong, China
[4] Bioland Laboratory (Guangzhou Regenerative Medicine and Health Guangdong Laboratory), Guangzhou, Guangdong, China
[5]Department of Obstetrics and Gynecology, Guangdong Provincial Key Laboratory of Major Obstetric Diseases, Key Laboratory of Reproduction and Genetics of Guangdong Higher Education Institutes, The Third Affiliated Hospital of Guangzhou Medical University, Guangzhou, Guangdong, China
[6]Center for Reproductive Medicine, Department of Obstetrics and Gynecology, Nanfang Hospital, Southern Medical University, Guangzhou, Guangdong, China
[7]Center for Reproduction, Affiliated Dongguan Hospital, Southern Medical University (Dongguan People's Hospital), Dongguan, Guangdong, China
[8]Department of Cell Biology, School of Basic Medical Sciences, Southern Medical University, Guangzhou, Guangdong, China

***Correspondence:** Xiangjin Kang, Department of Obstetrics and Gynecology, Guangdong Provincial Key Laboratory of Major Obstetric Diseases, Key Laboratory of Reproduction and Genetics of Guangdong Higher Education Institutes, The Third Affiliated Hospital of Guangzhou Medical University, Guangzhou, Guangdong, China. E-mail: xiangjinkang@gzhmu.edu.cn; Yong Fan, Department of Obstetrics and Gynecology, Guangdong Provincial Key Laboratory of Major Obstetric Diseases, Key Laboratory of Reproduction and Genetics of Guangdong Higher Education Institutes, The Third Affiliated Hospital of Guangzhou Medical University, Guangzhou, Guangdong, China. E-mail: yongfan011@gzhmu.edu.cn; Xiaochun Bai, Department of Cell Biology, School of Basic Medical Sciences, Southern Medical University, Guangzhou, Guangdong, China. E-mail: bxc15@smu.edu.cn; Zhenguo Chen, Guangdong Provincial Key Laboratory of Construction and Detection in Tissue Engineering, Department of Cell Biology, School of Basic Medical Sciences, Southern Medical University, Guangzhou, Guangdong, China. E-mail: czg1984@smu.edu.cn (Lead Contact)

[†]These authors contributed equally to this work.

Abstract

In mammals, testis development is triggered by the expression of the sex-determining Y-chromosome gene *SRY* to commit the Sertoli cell (SC) fate at gonadal sex determination in the fetus. Several genes have been identified to be required to promote the testis pathway following *SRY* activation (i.e., SRY box 9 (*SOX9*)) in an embryo; however, it largely remains unknown about the genes and the mechanisms involved in stabilizing the testis pathway after birth and throughout adulthood. Herein, we report postnatal males with SC-specific deletion of *Raptor* demonstrated the absence of SC unique identity and adversely acquired granulosa cell-like characteristics, along with loss of tubular architecture and scattered distribution of SCs and germ cells. Subsequent genome-wide analysis by RNA sequencing revealed a profound decrease in the transcripts of testis genes (i.e., *Sox9*, *Sox8*, and anti-Mullerian hormone (*Amh*)) and, conversely, an increase in ovary genes (i.e., LIM/Homeobox gene 9 (Lhx9), Forkhead box L2 (Foxl2) and Follistatin (Fst)); these changes were further confirmed by immunofluorescence and quantitative reverse-transcription polymerase chain reaction. Importantly, co-immunofluorescence demonstrated that *Raptor* deficiency induced SCs dedifferentiation into a progenitor state; the *Raptor*-mutant gonads showed some ovarian somatic cell features, accompanied by enhanced female steroidogenesis and elevated estrogen levels, yet the zona pellucida 3 (ZP3)-positive terminally feminized oocytes were not observed. In vitro experiments with primary SCs suggested that Raptor is likely involved in the fibroblast growth factor 9 (FGF9)-induced formation of cell junctions among SCs. Our results established that Raptor is required to maintain SC identity, stabilize the male pathway, and promote testis development.

Summary Sentence
Raptor deletion induced Sertoli cells into an undifferentiated state and showed some ovarian somatic cell features.

Received: December 24, 2021. **Revised:** April 21, 2022. **Accepted:** May 9, 2022

Graphical Abstract

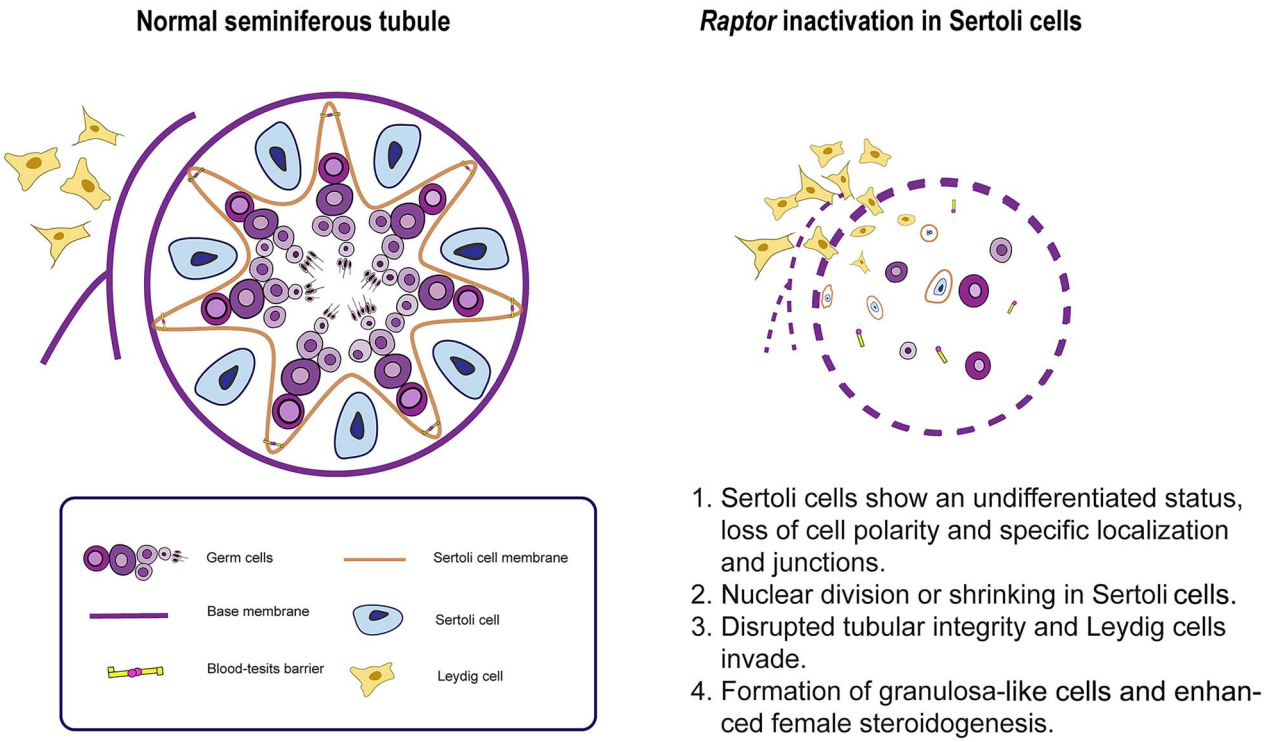

Keywords: Raptor, Sertoli cell differentiation, testis development, dedifferentiation, granulosa cell

Introduction

In mammals, the testis and ovary differentiate from an embryonic bipotential gonad. However, the testis appears to have a differentiating priority due to the presence of the sex-determining gene *SRY* on the Y chromosome [1, 2]. In mice, *Sry* is transiently expressed in XY progenitor cells from embryonic day 10.5 (E10.5)–E12.5, soon after the gonad is first formed [3, 4]. *Sry* predominantly and directly activates SOX9 [5]. SOX9 stimulates the expression of *Pgds* [6], which in turn amplifies SOX9 activity synergistically with FGF9 [7–9], further inducing differentiation of supporting cell lineages to the Sertoli cell (SC) fate and establishing the testicular cords. It has been recently demonstrated that expression of *Sry* is controlled by the epigenetic machinery by specific transcription factors, and epigenetic regulation plays an important role in gonadal sex determination [10, 11]. In the absence of *Sry* or *Sox9* activation, granulosa cell fate and ovary pathway are initiated, mainly involving the R-spondin1 (RSPO1)/WNT4-β-catenin signaling pathway [12–14], in coordination with FOXL2 [15–17] and Follistatin [18]. Other established pro-testis genes include *Dhh* [19], *Pdgfrα* [20], *Wt1* [21], *Cbx2* [22], as well as *Nr0b1/Dax1* [23], which was initially classified as a pro-ovary gene [24]. RUNX1 and COUP-TF2 were the two newly identified pro-ovary proteins [25, 26].

The gene expression patterns underlying initial sex differentiation suggest that some testis-specific genes are exclusively activated in the XY gonad, whereas alternately suppressed in the XX gonad at sex determination, and vice versa. It would be important to maintain such a gene activation/suppression mechanism throughout adulthood, as both terminally differentiated Sertoli and granulosa cells have the potential to mutually transform long after sex commitment. In support of this, loss of *Foxl2* in adult mouse ovaries led to reprogramming of granulosa cells into Sertoli-like cells along with the formation of a testicular cord-like structure [17]. In contrast, conditional deletion of the pro-testis gene *Dmrt1* in adult mouse testes resulted in transdifferentiation of SCs into granulosa cells accompanied by ovarian reorganization [27]. These reports highlight the susceptibility of gonadal sex reversal and indicate that sex-associated genes should be strictly monitored to ensure the destined testis or ovary pathway, even long after commitment in fetal life. However, relative to the initial stage of sex determination in the fetus, it largely remains unknown about gonadal sexual maintenance from the postnatal stage to adulthood, particularly in terms of the genes and mechanisms involved.

The mechanistic target of rapamycin (mTOR) is a highly conserved serine/threonine kinase that nucleates two distinct multiprotein complexes: mTOR complex 1 (mTORC1) and mTORC2 [28]. mTORC1 is a sensitive target of rapamycin and includes mTOR, regulatory associated protein of mTOR (Raptor), and other components, in which Raptor acts as a scaffold for recruiting mTOR substrates. Rheb is a direct upstream activator of mTORC1, which is suppressed by TSC1/2, a functional complex with GTPase-activating protein activity for Rheb [28]. mTORC1 integrates diverse signals, including nutrients, growth factors, energy, and stresses, to regulate cell growth, proliferation, survival, and metabolism [29]. In contrast, mTORC2 is insensitive to rapamycin and mainly contains the rapamycin-insensitive subunit, Rictor [28].

The central roles of the mTOR complex in growth, metabolism, autophagy, aging, and disease have been well established [29–31]. Recently, increasing evidence from us and other groups has demonstrated the critical roles of mTORC1/2 in regulating spermatogonial population homeostasis [32, 33] and SC function [34–37], suggesting its importance in testis development and spermatogenesis. Interestingly, a recent study with conditional knockout of *mTOR* in primordial follicles reported granulosa-to-SC transdifferentiation and follicle-to-testicular cord conversion in adult mutant ovaries [38], indicating normal mTOR signaling activity is required for the maintenance of granulosa fate and oogenesis. This study showed that mutant mice with conditional knockout of *Raptor* in SCs (SC*Raptor*KO) exhibited a profound change in SC morphology, accompanied by disrupted tubular structure and complete loss of testicular cell architecture. To gain more insight into the alteration of molecular networks underlying this change, we performed a genome-wide gene expression analysis by RNA sequencing (RNA-seq) of the control and SC*Rapto*KO testes. Interestingly, the data indicated dedifferentiation in SCs upon loss of *Raptor*.

Materials and methods

Mice

The details of generating the mutant mice with SC-specific knockout of *Raptor* (SC*Raptor*KO) and their control mates by mating the *Amh*-Cre and the *Raptor*$^{LoxP/LoxP}$ mice had been described in our previous study [35]. Eight-week-old wild-type (WT) female C57BL/6J mice were from the Medical Animal Center of the Southern Medical University. All the animal experiments were approved by the Southern Medical University Committee on the Use and Care of Animals and were performed following the Committee guidelines and regulations.

Hematoxylin and eosin, immunofluorescent staining, and transmission electron microscopy

Testes were fixed in modified Davidson fixative, processed in paraffin, and sectioned using standard procedures. At least three sections from each testis (5 μm, taken 100 μm apart) were stained with hematoxylin and eosin (H&E) for regular histological examination.

Immunofluorescent staining was performed according to a standard procedure, using the primary antibodies summarized in Supplementary Table S3 and the Alexa-Fluor-488- or Alexa-Fluor-594-labeled secondary antibodies (Jackson Immunoresearch, West Grove, PA, USA). 4,6-diamidino-2-phenylindole was used to visualize the nuclei. Immunofluorescent images were obtained using a FluoView FV1000 confocal microscope (Olympus, Shinjuku-ku, Tokyo, Japan).

Testis samples were fixed in 2% glutaraldehyde at room temperature for 2 h, and processed under a transmission electron microscope (TEM, H-7500, Hitachi, Chiyoda-ku, Tokyo, Japan).

Quantitative reverse-transcription polymerase chain reaction

Total testicular RNA was purified using the Trizol Reagent (Invitrogen, Carlsbad, CA, USA), and processed to cDNA using the Hifair™ II 1st Strand cDNA Synthesis Kit, followed by amplification and quantification using the Hieff® qPCR SYBR Green Master Mix (all from YEASEN Biotech Co. Ltd, Shanghai, China) with a StepOne Plus Real-Time PCR System (Applied Biosystems, Waltham, MA, USA). *Gapdh* was used as the endogenous control transcript. Three technical replicates were applied for each transcript. The primer sequences are summarized in Supplementary Table S4.

Enzyme-linked immunosorbent assay

Adult mouse gonads were homogenated in cold saline on ice. After centrifuging at 12 000 rpm at 4°C for 15 min, the supernatant was collected for testosterone and estradiol measurement by using the enzyme-linked immunosorbent assay (ELISA) kits (testosterone, E-EL-0072c, detection level: 0.10–20 ng/ml; estradiol, E-EL-0150c, 9.37–600 pg/ml; both from Elabscience, Wuhan, China). The values are normalized by protein concentrations and present as ng/mg protein and pg/mg protein, respectively.

Ultra performance chromatography-tandem mass spectrometry analysis for steroid measurement

A 50 mg aliquot of each individual sample was weighed and 200 μl distilled water was added, two small steel balls and homogenated three times. After adding 500 μl of extract solution methanol and 40 μl internal standard, the samples were vortexed. Then 600 μl water was added and vortexed again. After centrifugation (5 min, 13 000 rpm, and 4°C), a 700 μl aliquot of the supernatant was transferred to an Eppendorf tube. The sample was further purified with Positive Pressure 96 Processor and then was collected into the 96-hole collecting plate. After being mixed in the micro-hole plate constant temperature vibrator, the sample was subjected to ultra performance chromatography-tandem mass spectrometry (UPLC-MS/MS) analysis. The UPLC separation was carried out using an ACQUITY UPLC-I/CLASS (Waters, Milford, MA, USA), equipped with an XBridge® BEH C8 (100 × 2.1 mm, 2.5 μm, Waters). The auto-sampler temperature was set at 10°C, and the injection volume was 10 μl. MassLynx Work Station Software (Version 4.1) was employed for MRM data acquisition and processing.

Western blotting

Testes were triturated and lysed on ice with radio immunoprecipitation assay (RIPA) lysis buffer. After centrifugation at 12 000 rpm at 4°C, the supernatant was collected and boiled in sodium dodecyl sulfate (SDS) loading buffer. Protein extracts were then subjected to 6–12% SDS-polyacrylamide gel electrophoresis and electrotransferred to nitrocellulose membranes (10 600 001, GE Healthcare Life Sciences). The membranes were then blocked in 5% nonfat dry milk for 1 h at room temperature, washed, and incubated with a primary antibody at 4°C overnight. The membranes were further washed, incubated with horseradish peroxidase-conjugated secondary antibody (111-035-003, 115-035-003, Jackson Immunoresearch) for 1 h at room temperature, washed again, and finally visualized using an enhanced chemiluminescence kit (NEL105001EA, PerkinElmer, Waltham, MA, USA). Quantification was performed by measuring the gray value of bands using the Image J software (1.52a, National Institutes of Health, USA).

RNA sequencing and differential analysis

5-dpp-old control and SC*Raptor*KO testes were used for total RNA isolation using TRIzol reagent. After quality control, RNA-seq was performed as digital gene expression on an Illumina HiSeq 2500 platform (RiboBioCo. Ltd, Guangzhou, China). Significant differences were analyzed by negative binomial distribution test after read-counts normalization, fold change, and adjusted *P* value (*Q* value) by the Benjamini-Hochberg false discovery rate procedure (*Q* value) were considered as factors for differential analysis. Control and SC*Raptor*KO testes RNA-seq data have been deposited in the NCBI SRA database (PRJNA767807). WT ovary sequencing data were downloaded from https://www.ncbi.nlm.nih.gov/geo/ (GSM5184147, GSM5184148).

Primary SCs isolation, culture, and treatment

Immature SCs were isolated from 5-dpp-old WT C57BL/6J mice as previously described with minor modification [39]. Briefly, decapsulated testes were minced into small fragments and incubated at 37°C for 15 min with collagenase A (1 mg/ml) in Dulbecco's modified Eagle's medium (DMEM)/12 with L-glutamine plus 15 mM 2-[4-(2-Hydroxyethyl)-1-piperazinyl]ethanesulfonicacid (HEPES) and DNase (20 μg/ml). Subsequently, cells were dispersed by incubation with (2 mg/ml) collagenase A, hyaluronidase (2 mg/ml), and DNase (20 μg/ml) (all from Sigma-Aldrich, Shanghai, China) in DMEM/F12 with L-glutamine plus 15 mM HEPES at 34°C for 30 min. Enzymatic digestions were stopped by brief treatment with soybean trypsin inhibitor (400 μg/ml) in DMEM/F12 supplemented with 2 mg/ml BSA. The cell suspension was centrifuged for 45 s at $50 \times g$. The pellets contain SCs and germ cells and were further digested with (2 mg/ml) collagenase A, (2 mg/ml) hyaluronidase, and (20 μg/ml) DNase in DMEM/F12 for 20 min at 34°C. Cell clusters were gently dispersed by homogenization using a potter. The cell suspension was filtered through a sterile (70 μm pore size) nylon mash. The cells were cultured in DMEM/F12 supplemented with 2 mM L-glutamine, 100 U/ml penicillin, 100 μg/ml streptomycin, 10 ng/ml epidermal growth factor (C600056, Sangon, Shanghai, China), 5 μg/ml human transferrin (T8158, Sigma-Aldrich), 2 μg/ml insulin (91077C, Sigma-Aldrich), 10 nM testosterone (HY-15554A, MedChem Express, Shanghai, China), 100 ng/ml follicle-stimulating hormone (8576-FS-010, R&D, Minneapolis, MN, USA), and 3 ng/ml cytosine arabinoside (C1768, Sigma-Aldrich). Cells were seeded at a density of $1–2 \times 10^7$ onto 100 mm^2 Matrigel-covered dishes and incubated at 34°C in a humidified atmosphere containing 5% CO_2 and 95% air. To remove germ cells and increase the purity of the SCs preparation, after 3 days of culture, the SC monolayer was subjected to hypotonic shock by incubation with 20 mM Tris–HCl (pH 7.5) for 5 min at room temperature. The hypotonic solution was replaced with a medium (lacking cytosine arabinoside). The medium was exchanged every day and the SCs used for experiments after 4 days of cultures. The identity of these cells as SCs was based on immunostaining for vimentin. The purity of the SC cultures was higher than 95%.

For experiments, SCs were seeded at greater than 90% confluent then transfected with negative control or *Raptor*-targeting siRNA via Lipofectamine 3000 (Invitrogen). 12 h later, cells were starvated with DMEM/F12 only without any growth factors. 24 h later, cells were treated with human FGF9 (20 nM in DMEM/F12, C198, Novoprotein, Shanghai, China) for another 24 h and finally collected for indicated analyses.

Statistical analysis

All experiments were performed in triplicate. Data are expressed as mean values ± standard errors, and differences between groups were analyzed by the *t*-test (SPSS 13; SPSS, Chicago, IL, USA). $P < 0.05$ was considered statistically significant.

Results

Deletion of *raptor* in SCs disrupted testicular organization and cell architecture

Histomorphological examinations showed that the SC*Raptor* KO tubules displayed age-dependent degeneration. By 60 dpp, most SC*Raptor*KO tubules were collapsed, characterized by the absence of tubular cell hierarchy and veil-like cytoplasmic extensions pointing toward the lumen and expansion of interstitia (Figure 1A). As SCs are the central organizer of the testicular architecture, we focused on the effects of *Raptor* deletion on SCs. Immunofluorescence of Wilms tumor 1 (WT1), an SC nuclei marker, showed that *Raptor*-deficient SCs did not align along the basement membrane but dispersed in the seminiferous epithelia compared with control mature SCs (Figure 1B). Transmission electron microscopy images further confirmed that *Raptor*-deficient SCs lost typical tripartite nucleoli, veil-like cytoplasmic extensions, and intrinsic cell junctions and had a distinct nucleic morphology; they were detached from the basement membrane (Figure 1C). These changes might indicate an immature configuration in the *Raptor*-deficient SCs. Notably, gap junction protein GJA1 exhibited a regular and continuous distribution in the control testes, whereas in the SC*Raptor*KO testes, a discontinuous distribution at 15 dpp and a severely disrupted and dot distribution in adulthood were observed (Figure 1D). This resembled its counterpart among granulosa cells in the adult WT ovary (Figure 1D). When calculating the ratio of the short to the long axis of the adult SC*Raptor*KO testes, we found that it was close to that of adult WT ovaries (Supplemental Figure S1). These observations together suggested that *Raptor*-deficient SCs lost their mature characteristics and may present an immature state, thus disrupting testis development.

Loss of *raptor* induces SCs into an undifferentiated state

To define the extent of dedifferentiation of the *Raptor*-mutant SCs and explore the possibility of undifferentiated SCs reversing into ovarian somatic cells, we performed whole-transcriptome sequencing and analyses of control and SC*Raptor*KO testes mice at 5 dpp when tubular morphological changes were initiated but without sharp degeneration. This revealed a large gene set upregulated in the *Raptor*-mutant testes, and surprisingly many of them were expressed in common between *Raptor*-mutant testes and WT ovaries (Figure 2A). We observed many genes upregulated were involved in sex-related biological processes, including male and female gonad development, sex somatic cell fate determination, response to estrogen, and regulation of canonical WNT signaling (Figure 2B). Of note, the genes characteristic of testicular Sertoli and Leydig cells and

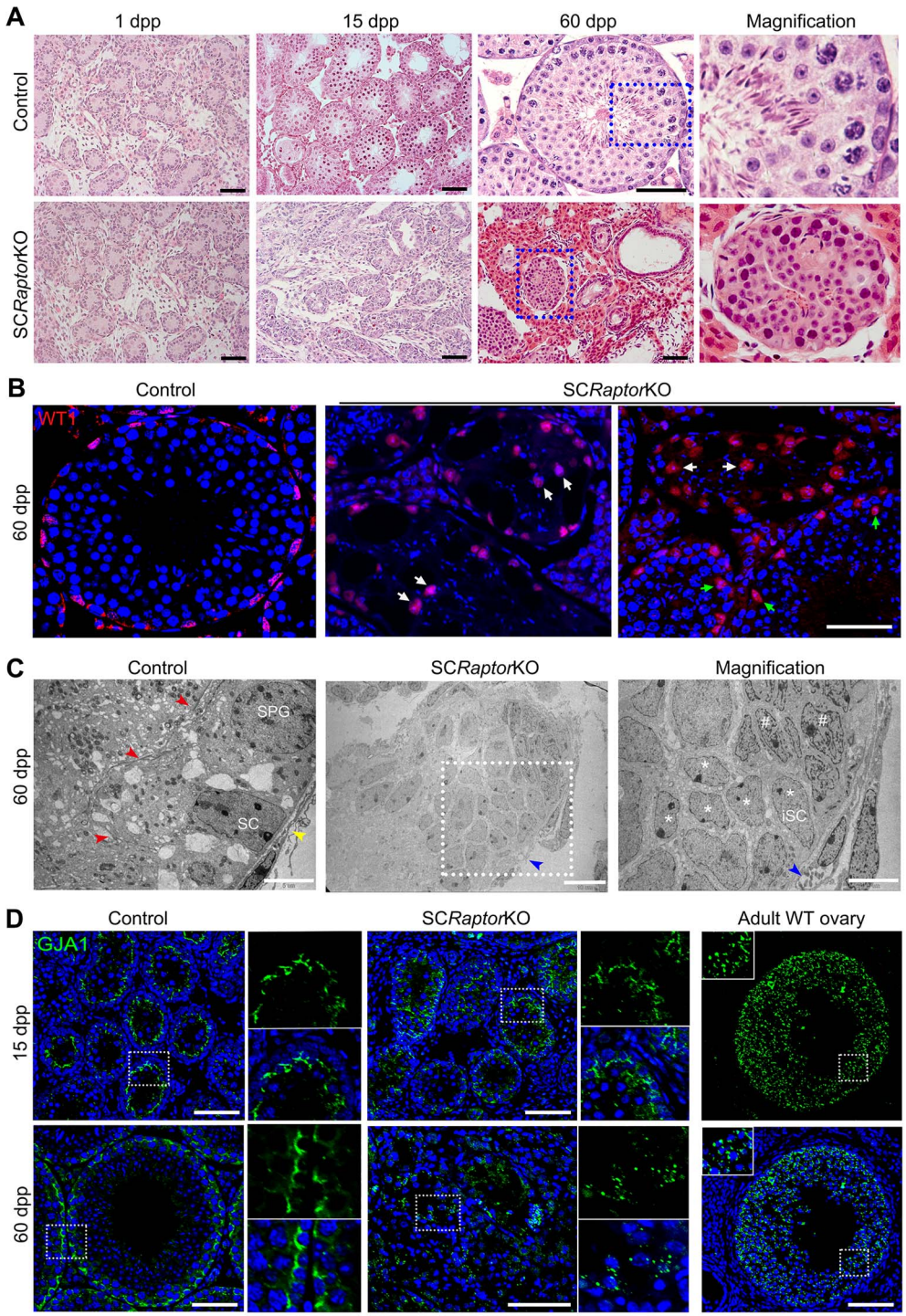

Figure 1. Testicular organization and cell architecture were impaired in SC*Raptor*KO males. (A) H&E staining showed age-dependent degeneration of tubules in the mutant testes. (B) Immunofluorescence of WT1, a SC nucleic marker, in the adult control and mutant testes. White arrowheads denote aberrant SC location in heavily damaged tubules losing most germ cells; green arrowheads denote aberrant SC location in relatively intact tubules. (C) TEM images showed a loss of SC characteristics in the adult mutant testes. Red arrowheads indicate intact cell junctions between adjacent SCs and between Sertoli and germ cells, yellow arrowheads denote intact contact between peritubular myoid cells in the control testes, and blue arrowheads denote discontinuous myoid cell layers in the mutant testes. * indicates immature Sertoli cells (iSCs); # indicates degenerated SCs with shrinking or fragmented nuclei. (D) Immunofluorescence of the gap junction protein GJA1 in the control and mutant testes at indicated ages. Images from an adult WT ovary were included for comparison. Scale bars = 50 μm in (A) and (C), 100 μm in (D), and 10 μm for low magnification and 5 μm for high magnification in (B).

essential for testis development and function, i.e., *Sox9*, *Sox8*, *Amh*, *Clu*, *Dhh*, *Gata1*, *Inha*, *Hsd17b3*, and *Cyp26b1* [19, 40–46], were significantly downregulated, while the genes well-characterized as ovary markers, i.e., *Foxl2*, *Lhx9*, *Fst*, *Esr2*, and *Cyp1b1* [16, 18, 47–49], were significantly upregulated (Figure 2B; Dataset S1). Among the most significantly enriched Gene Ontology (GO) terms associated with the altered transcripts were "cell adhesion", "regulation

of cell proliferation", "regulation of apoptotic process", "regulation of gene expression", and "cell differentiation" (Figure 2C). The top GO term "cell adhesion" was of the highest significance and associated with numerous transcripts. These data demonstrated the loss of unique SC characteristics upon loss of *Raptor* and simultaneously indicated a general activation of the ovarian genes.

Using single-cell RNA seq of *Nr5a1*-expressing gonadal somatic cells [50], Stévant et al. deconvoluted the gene expression dynamics during three categorized periods of supporting cell lineage specification, namely: stage a, XY/XX early progenitor cells; stage b, pre-Sertoli/pre-granulosa cells; and stage c, Sertoli/granulosa cells. We then compared all the genes detected in our sequencing data with all in the Stévant, aiming to (1) determine the extent of dedifferentiation in gonadal somatic cell lineages and (2) explore the possibility of gonadal sex reprogramming in the *Raptor*-mutant testes. We found 204 genes in common (Figure 2D). In the *Raptor*-mutant testes, two XX early progenitor cell markers (*Ibsp* and *Cnr1*), four pre-granulosa cell markers (*Lhx9*, *Thsd7b*, *Fgfr2*, and *Fst*), and 43 granulosa cell markers were markedly upregulated, while seven XY early progenitor cell markers, five pre-SC markers, and 114 mature SC markers were markedly downregulated (Figure 2D; Dataset S2). These data globally suggested downregulation of the mature SC markers whereas upregulation of the markers for ovarian mature and somatic progenitor cells in the *Raptor*-mutant testes, reminiscent of dedifferentiation of *Raptor*-mutant SCs.

Expression of LHX9, but not FOXL2, was increased in SC*Raptor*KO testes

To further validate the RNA-seq data and examine the possible gonadal somatic cell fate transition, we performed immunofluorescent staining of LHX9, expressed in progenitor cells for both SCs and granulosa cells [51, 52]. LHX9 was strongly expressed in XX gonads at E12 when supporting cell commitment is undergoing and then largely decreased at E14.5 when cell commitment is complete. In the XY gonad, the LHX9 level was lightly detectable (Figure 3A). These results are consistent with previous reports. Based on this, we characterized expression profiles in paired testes from 5 to 60 dpp, which showed that LHX9 expression was robustly increased in the degenerating/degenerated tubules in the SC*Raptor*KO testes in an age-dependent manner (Figure 3B). We then profiled the expression of another granulosa cell marker, FOXL2, which is required for ovary commitment, and its deficiency in adult ovaries triggers a testis-like reorganization [16, 17]. Quantitative reverse-transcription polymerase chain reaction (qRT-PCR) analysis revealed a striking elevation of *Foxl2* mRNA level in the SC*Raptor*KO testes, validating its change in the sequencing data. An elevation of *Wnt4* while downregulation of *Dmrt1* was also observed in the SC*Raptor*KO testes. Unexpectedly, we only observed a subtle increase in the FOXL2 protein level in the SC*Raptor*KO testes (Supplemental Figure S2), indicating that FOXL2-positive terminal mature granulosa cells were not induced in the SC*Raptor*KO testes. Alternatively, there might be a post-transcriptional regulation. These results provided evidence that the markers for ovarian somatic progenitor or granulosa cells are upregulated in the SC*Raptor*KO testes.

Raptor-deficient SCs exhibit some features resembling ovarian granulosa cells and are functional in producing estrogen

We observed that a Leydig cell marker 3β-HSD2, a key enzyme in testosterone synthesis, was largely upregulated in the *Raptor*-mutant testes (Supplemental Figures S3 and S4). We previously thought this might be a negative feedback phenomenon due to impaired SC function. It is noteworthy that both adult Leydig and theca cells are thought to be recruited from surrounding progenitor populations [53, 54]. In the ovary, granulosa cells produce estrogen, and theca cells are induced during follicle growth, likely by signals from granulosa cells. Together with oocytes, these three comprise the functional unit of the ovary. Therefore, we asked whether *Raptor*-deficient SCs can be transdifferentiated into ovarian somatic cells (e.g., granulosa cell), whether they were functional (e.g., producing estrogen), and whether oocytes were formed. To this end, we performed immunofluorescent staining of aromatase/CYP19α1, an enzyme in granulosa cells important for estrogen synthesis that catalyzes testosterone to estradiol, as well as 3β-HSD2, which is expressed in ovary theca cells (Supplemental Figure S4). α-smooth muscle actin (α-SMA) was also labeled to mark the base membrane. As expected, their expressions were robustly enhanced in the *Raptor*-mutant testes. More importantly, many signals were localized within the basement membrane (Figure 4A), contrary to their counterparts, which were restricted to the interstitium in the control testes. Interestingly, some aromatase-positive and 3β-HSD2-positive intratubular cells in the *Raptor*-mutant testes slightly resembled the WT ovary granulosa and theca cells (Figure 4A, inserts). We further performed co-immunofluorescence of aromatase and 3β-HSD2 with GATA-4, an SC marker, respectively, and found that aromatase/GATA-4 and 3β-HSD2/GATA-4 each co-localized in cells (Figure 4B, inserts). Some 3β-HSD2/GATA-4-positive cells appeared with a spindle shape analogous to WT theca cells (Figure 4B, arrowhead in the inserts). Furthermore, the progenitor cell marker LHX9 was also co-expressed with GATA-4 (Figure 4B). However, as Leydig cells also express 3β-HSD2 and most of the 3β-HSD2-positive intratubular cells were located in the tubules with disrupted tubular integrity (discontinued SMA expression, asterisks in Figure 4A), they could be derived from expanded Leydig cells that invaded the tubule remnants due to SC dysfunction. Overall, these results suggested some signs that *Raptor*-mutant SCs can be dedifferentiated into progenitor cells, which then turn to express enzymes required for ovarian somatic cell functions.

We next assessed female steroidogenesis by qRT-PCR analyses of the associated enzymes. The results revealed a significant elevation in the mRNA levels of estrogen associated enzymes (Supplemental Figure S4), including estrogen-producing *aromatase/Cyp19a1* and *Hsd17b1*, and estradiol-metabolizing *Cyp1a1* and *Cyp1b1*, as early as 5 dpp; these levels were further elevated at 15 dpp, although *Cyp1a1* and *Cyp1b1* decreased at 60 dpp (Figure 5A). Notably, when introducing age-match WT ovaries for comparison, we observed a similar expression pattern for most enzymes between the *Raptor*-mutant testes and the WT ovaries, especially for *aromatase*, *Cyp1a1*, and *Cyp1b1*. Consistent with these enzyme changes, an ELISA assay with whole gonad extracts showed that estradiol level was raised in the adult mutants relative to the adult controls (Figure 5B). The level

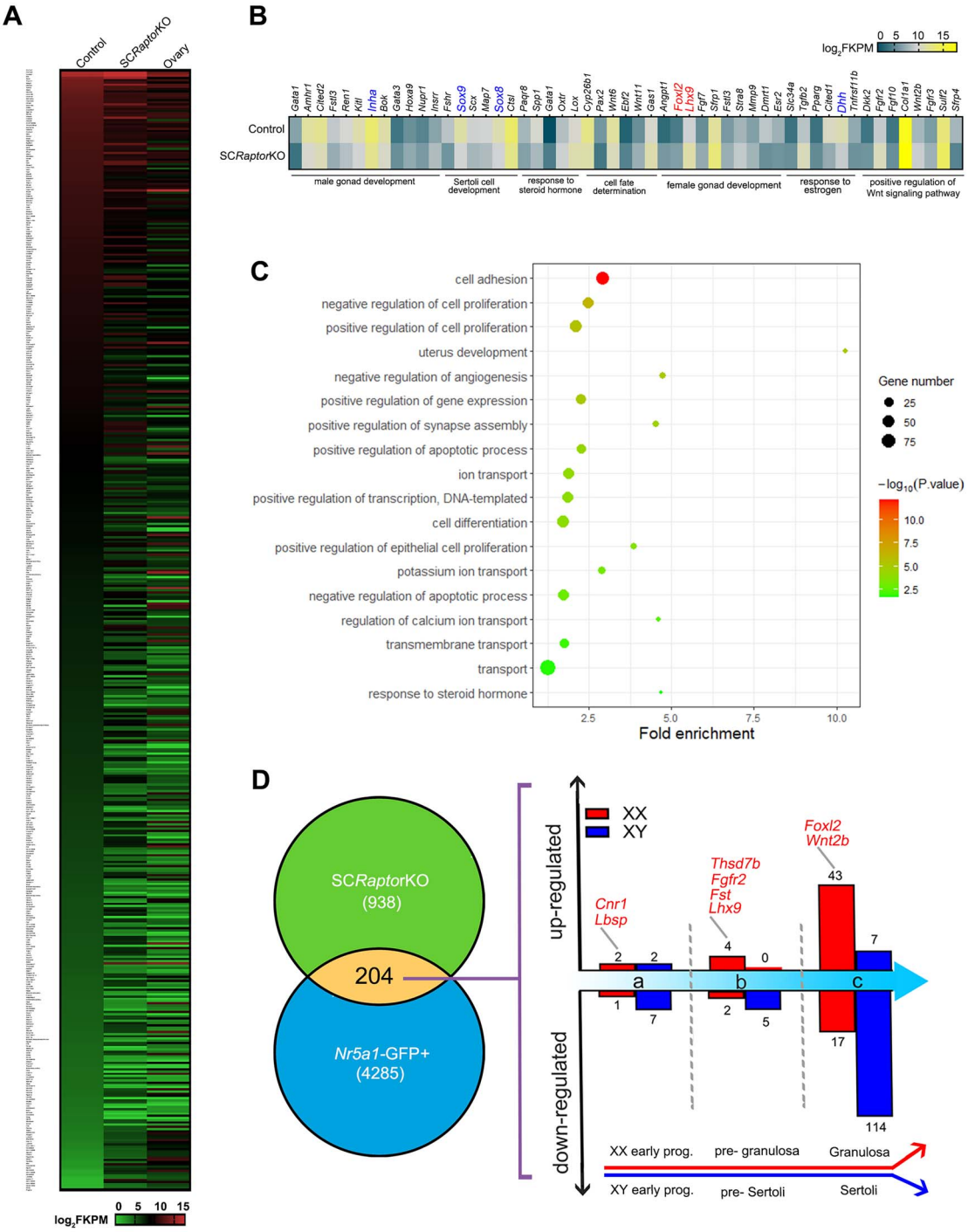

Figure 2. Molecular profiling of the genes associated with gonadal somatic cell differentiation in the SC*Raptor*KO testes. (A) Heat map showing all significantly changed transcripts identified by RNA-seq in the control and mutant gonads compared to WT ovaries (see Supplementary Table S1 for a complete list of transcripts). (B) Heat map illustrating differences between the control and mutant gonads in expressing a cohort of transcripts involved in various GO processes, which are tightly associated with sex determination and gonad development. Some well-established testis genes downregulated in the mutant gonads were marked in blue, and those ovary genes upregulated were marked in red. (C) Heat map revealing other enriched GO terms significantly associated with changed transcripts. (D) Venn diagram depicting the relationship of the altered transcripts in our RNA-seq data and previous single-cell RNA-seq data. Shown is also the distribution of the 204 transcripts among three cell lineage specification stages for gonadal somatic cells. The XX cell genes upregulated in the SC*Raptor*KO gonads are highlighted in red.

of androgenic enzyme *Hsd17b3* was increased after 15 dpp, and that of *Sr5d3*, which encodes 5-α-reductase that catalyzes testosterone to generate active dihydrotestosterone [55], was relatively steady in the mutants (Figure 5A). Nevertheless, the testosterone level in the mutant gonads was significantly decreased (Figure 5C). Shortages of 17-OH-progesterone and androstenedione (Figure 5D and E), the two last steroids in the testosterone synthesis pathway (Supplemental Figure S4),

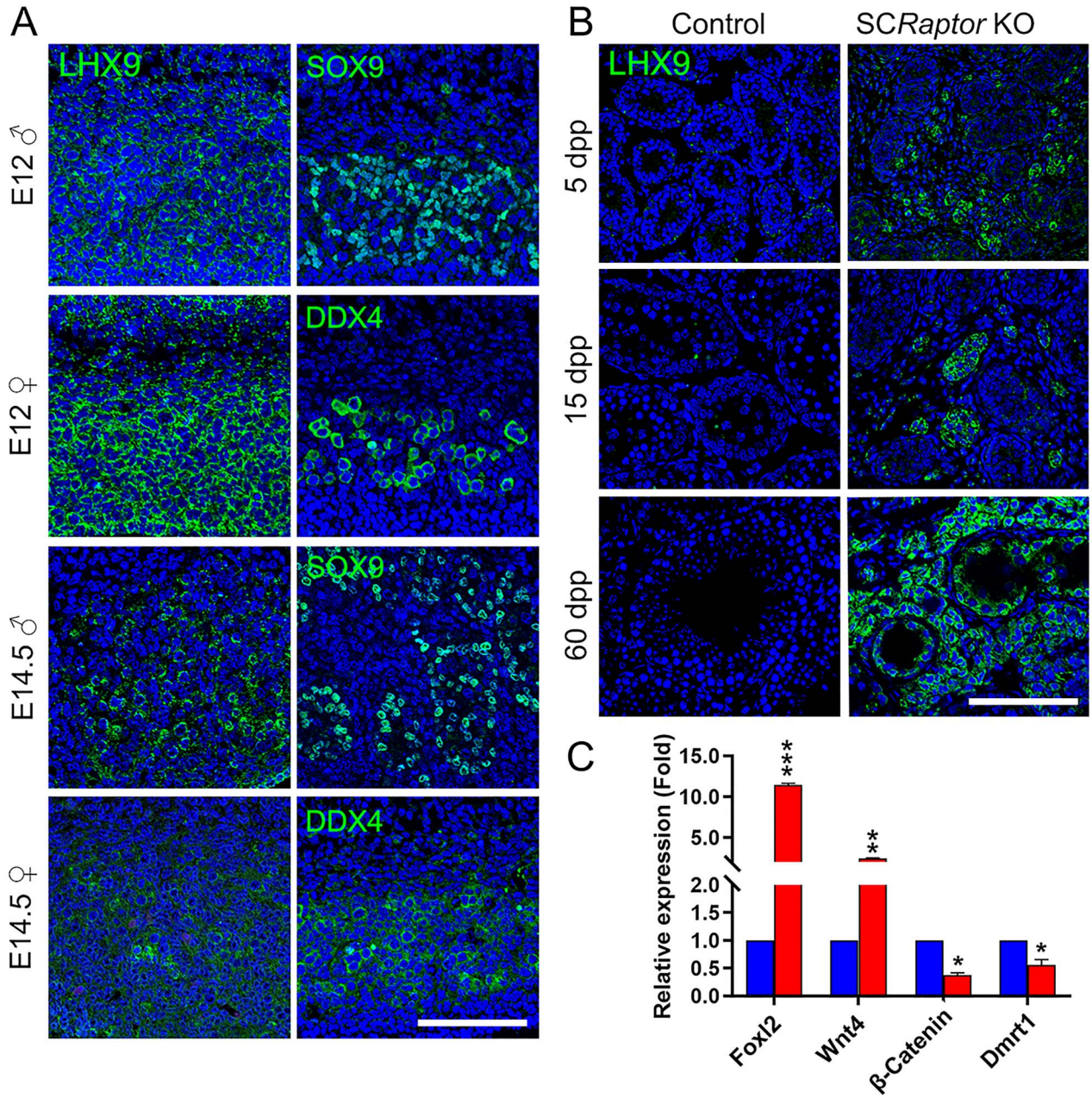

Figure 3. Expression of the somatic progenitor cell marker LHX9 and the pro-ovary protein RSPO1 was increased in the SC*Raptor*KO testes. (A) Immunofluorescent profile of LHX9 in WT male and female gonads at E12 and E14.5. SOX9 and DDX4 were used as the markers for male and female germ cells, respectively, to confirm the sex of mice. (B) Age-dependent elevation in protein levels of LHX9 in the *Raptor*-mutant testes revealed by immunofluorescence. (C) mRNA levels of indicated genes revealed by qRT-PCR. *, $P < 0.05$; **, $P < 0.01$; ***, $P < 0.001$. Scale bars = 100 μm.

primarily accounted for this decrease. We did not detect expression of the oocyte-specific zona pellucida protein ZP3 in the mutant XY gonads at any ages detected (Figure 5F), indicating male germ cells were not yet feminized. Overall, these data suggested that *Raptor*-deficient SCs present some ovarian somatic cell features and can produce estrogen.

Knockdown of *raptor* attenuates the promoting effects of FGFf9 on cell junctions among SCs

FGF9/FGFR2 signaling plays a crucial role in male sex determination [56]. GO analysis of our RNA-seq data also revealed that FGF signaling was associated with notable changes in transcripts. qRT-PCR analyses with the 5 dpp paired gonads confirmed that mRNA levels of *Fgf9* and *Flrt1* were downregulated, while those of *Fgf7*, *Fgfr2*, *Fgfr3*, and *Fat4* were upregulated and that of *Fgf10* was unchanged (Figure 6A). To determine whether Raptor was involved in FGF9 signaling, immature primary SCs were isolated from 5 dpp WT mouse testes, transfected with siRNA targeting *Raptor*, and treated with FGF9. qRT-PCR results showed that *Raptor* mRNA expression was effectively eliminated by the siRNA, but *Raptor* knockdown hardly changed mRNA levels of the detected FGF pathway members under physiological conditions (Figure 6B). Upon FGF9 stimulation, the mRNA levels of FGF pathway members were significantly raised,

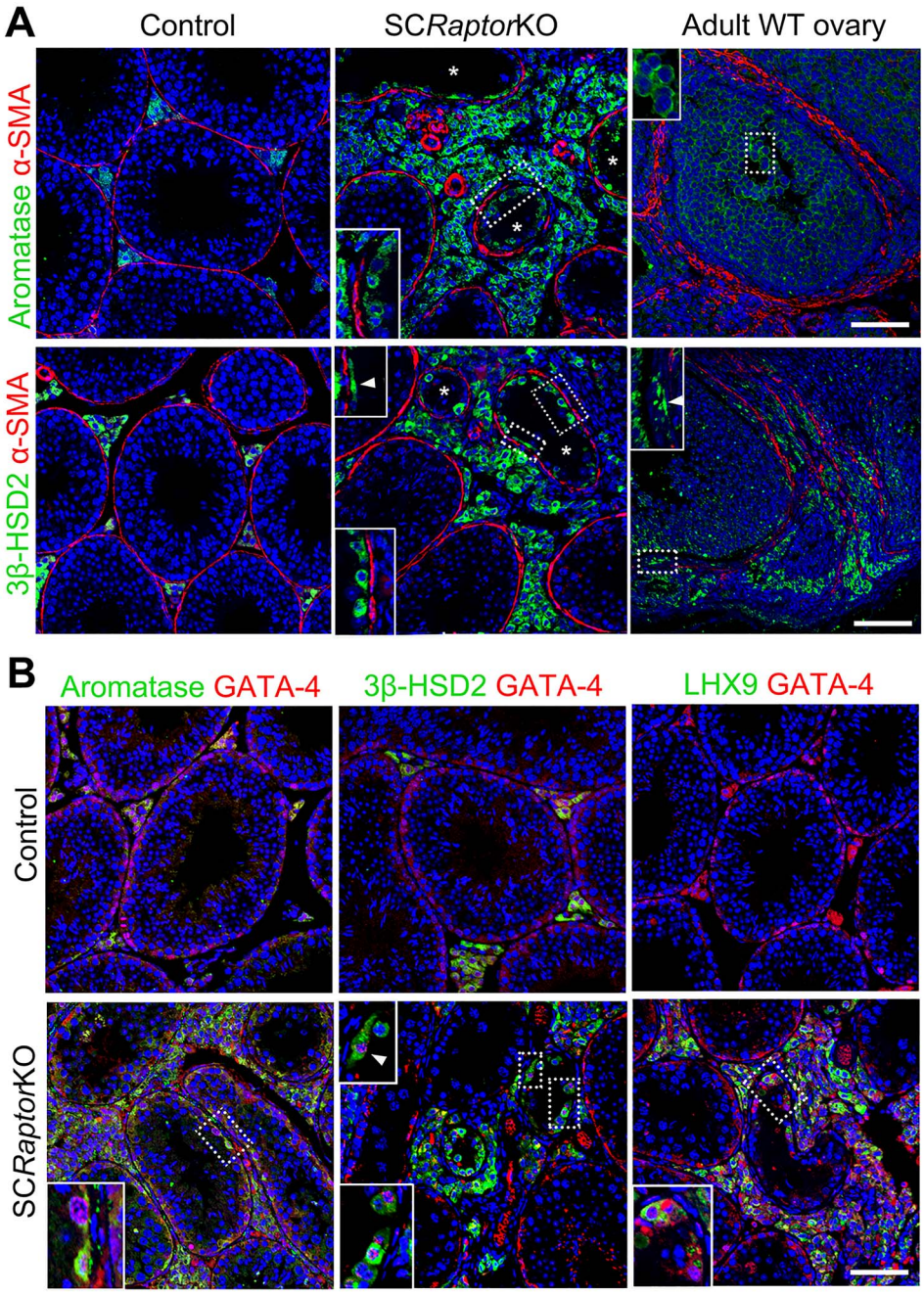

Figure 4. *Raptor*-mutant SCs express steroidogenic enzymes required for estrogen synthesis. (A) Co-immunofluorescence of aromatase/α-SMA and 3β-HSD2/α-SMA in the adult control and *Raptor*-mutant testes and the adult WT ovaries. (B) Co-immunofluorescence of aromatase, 3β-HSD2, and LHX9 with GATA-4, a SC nuclear marker, respectively, in the adult control and *Raptor*-mutant testes. Asterisks (*) denote the tubules with disrupted integrity. White arrowheads denote potentially transdifferentiated theca-like cells with a spindle shape in the adult *Raptor*-mutant gonads and normal theca cells in the adult WT ovaries. Scale bars = 100 μm.

which were counteracted by *Raptor* knockdown, although *Raptor* mRNA levels remained unchanged in response to FGF9 (Figure 6B). This indicated that *Raptor* downregulation attenuated FGF9 signaling in vitro. Formation of the blood-testis barrier (BTB) is widely accepted as a hallmark of SC maturation [36]. We next asked whether Raptor plays a role in the FGF9-driven formation of cell junctions among SCs. Immature SCs transfected with control or *Raptor*-siRNA were normalized in a basic medium and treated with FGF9. Western blotting showed that the protein levels of BTB-associated Cingulin, β-catenin, and ZO-2 were decreased in the knockdown group when cultured in a basic medium. FGF9 treatment enhanced their protein expression, while expression was attenuated by *Raptor* knockdown (Figure 6C). To confirm this further, we performed immunofluorescent staining. Consistent with our previous report showing aberrant Cingulin expression and distribution in the SC*Raptor*KO testes [35], *Raptor* knockdown also markedly decreased the cytoplasmic spreading of Cingulin, as well as its accumulation around the interacting boundary among primary SCs in response

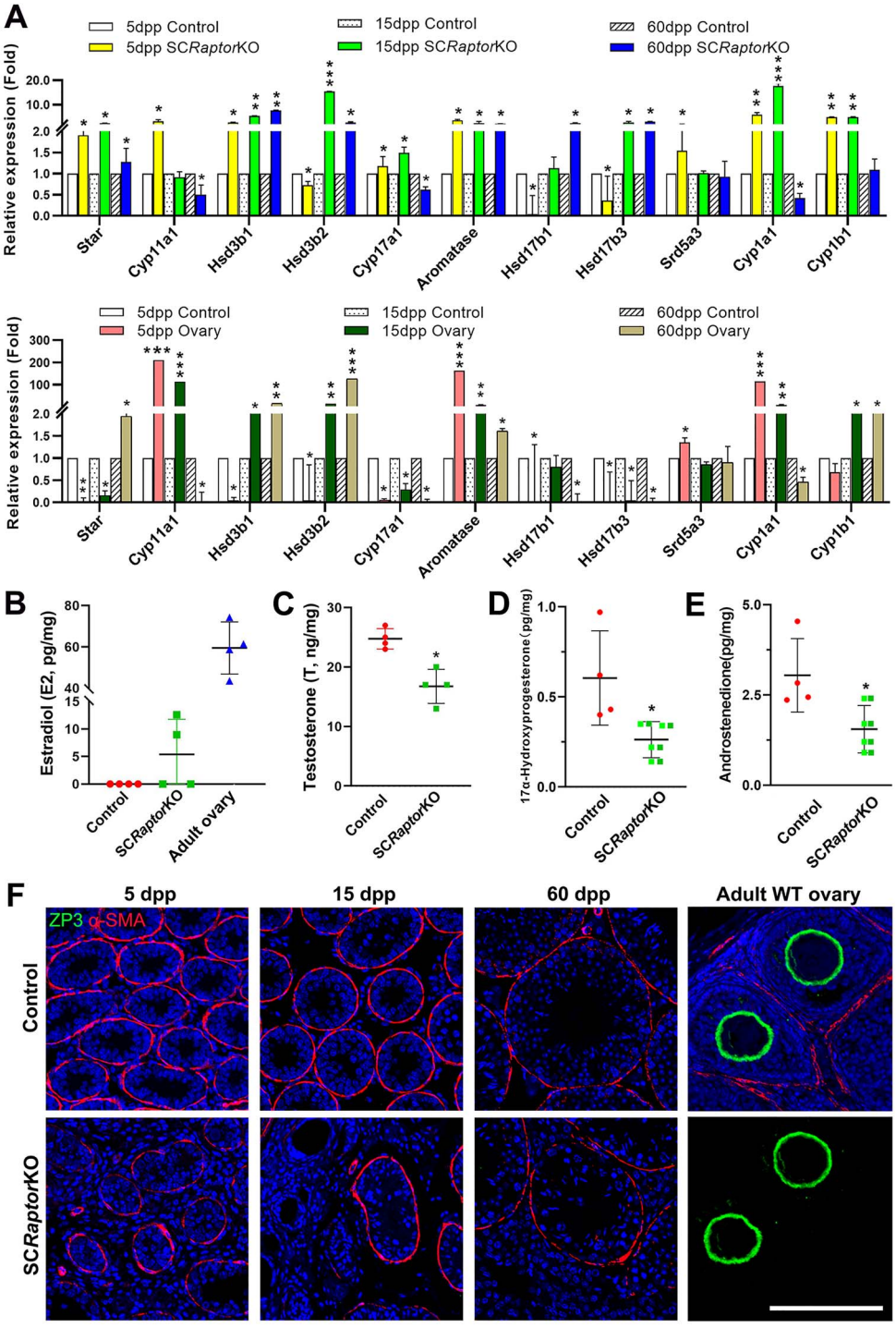

Figure 5. Female steroidogenic activity and estradiol levels were elevated in the SC*Raptor*KO gonads. (A) qRT-PCR shows the expression profiles of the enzymes involved in male and female steroidogenesis in control and mutant gonads from 5 to 60 dpp. Age-match WT ovaries were included for comparison. (B) Raised estradiol levels in the adult mutant gonads were revealed by ELISA. The data are present as pg per mg protein. Adult WT ovaries were also included for comparison. Note that all four control testes assayed had levels below the detection limit and thus were defined as zero, whereas two out of four mutant testes had measurable estradiol. (C) Reduced testosterone levels in the adult mutant gonads. The data are present as ng per mg protein. (D and E) Measurement of 17-OH-progesterone (D) and androstenedione (E) by UPLC-MS/MS. Both data are present as pg per mg tissue mass. (F) Co-immunofluorescence of α-SMA and ZP3, an oocyte-specific zona pellucida protein, in control and mutant gonads from 5 to 60 dpp and adult WT ovaries. *, $P < 0.05$; **, $P < 0.01$; ***, $P < 0.001$. Scale bar = 100 μm.

to FGF9 stimulation (Figure 6D). FGF9 treatment induced nucleus-to-cytoplasm transport of β-catenin and gathering in the contact areas among SCs; this was blocked by *Raptor* knockdown (Figure 6D). Similar results were observed with ZO-2. FGF9 treatment also induced cytoplasmic spreading of Vimentin, the SC intrinsic cytoskeleton protein, but it appeared unchanged after *Raptor* knockdown (Figure 6D). These data suggested that *Raptor* downregulation did not

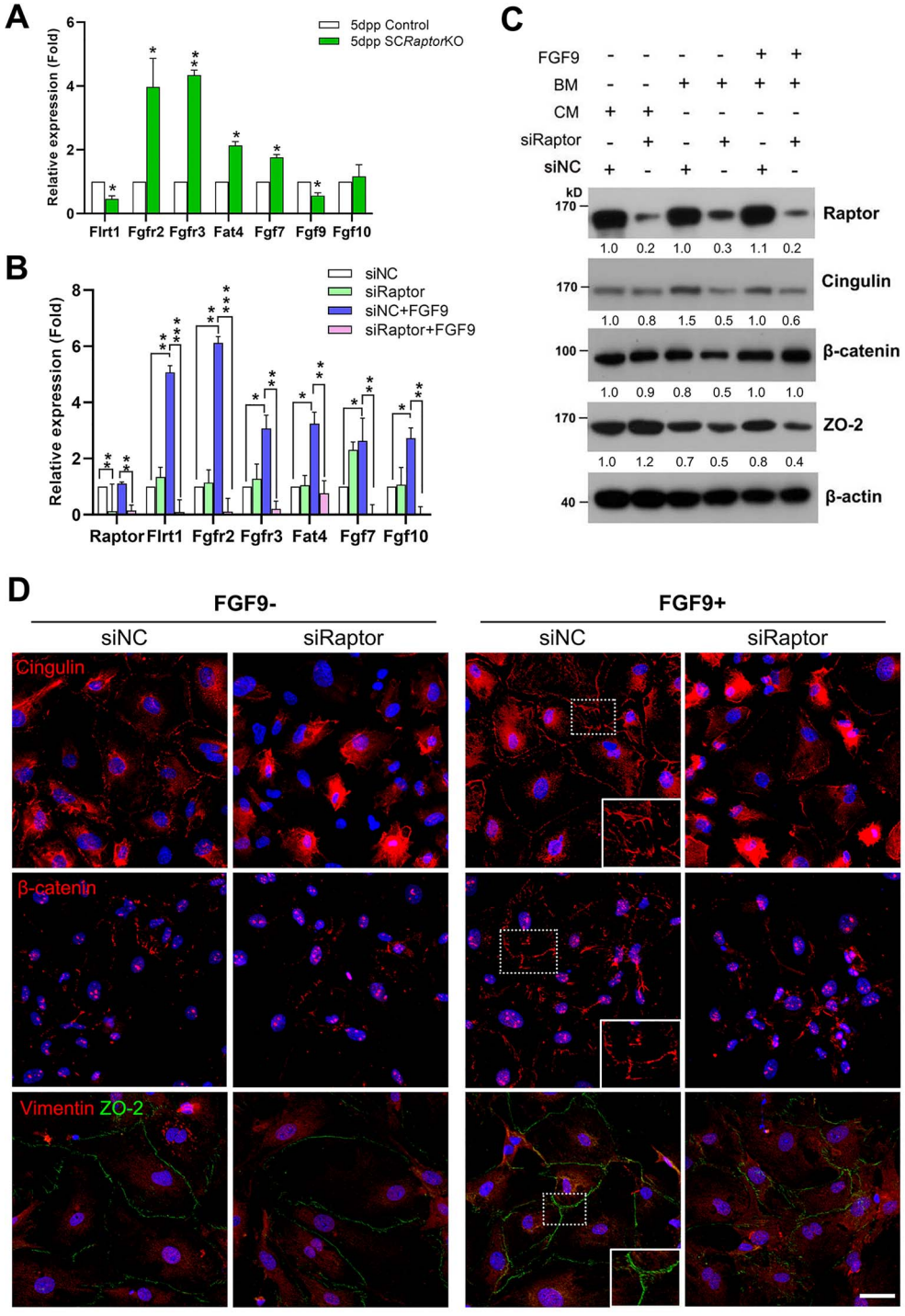

Figure 6. Knockdown of *Raptor* attenuated FGF9-induced establishment of cell junctions in primary SCs. (A) qRT-PCR analyses of the mRNA levels of FGF members in 5 dpp control and mutant gonads. (B) qRT-PCR analyses of the FGF member transcripts in primary SCs with *Raptor* knockdown in response to FGF9 stimulation. Immature primary SCs were isolated and treated as described in *Materials and methods*. (C) Western blotting analyses of the BTB-associated protein levels in primary SCs as treated in (B). Quantification of gray values was shown under bands. BM, basic medium without growth factors; CM, complete medium with all required growth factors. (D) Immunofluorescent analyses of the distribution of BTB-associated protein in (C). *, $P < 0.05$; **, $P < 0.01$; ***, $P < 0.001$. Scale bar = 50 μm.

affect the cytoskeletal organization in SCs, but disrupted the establishment of cell junctions among SCs by impairing the gathering and arrangement of BTB-related proteins. This may present a potential mechanism in which Raptor acts downstream of FGF9 signaling to promote SC maturation and maintain their identity.

Discussion

To our knowledge, this is the first report showing that one of the key components of the mTOR complex, more precisely, mTORC1, is essential for the maintenance of SC differentiation identity after birth. Its deficiency induced SCs dedifferentiation into a progenitor state, thus depriving SC

maturation characteristics, including specific cell junctions between SCs and between SCs and male germ cells, and unique nucleic morphology and cell location. We also observed that *Raptor*-mutant SCs exhibited some ovarian somatic cell-like features, including actively producing estrogens. Yet, we did not observe terminally feminized ZP3-positive follicles in the XY *Raptor*-mutant gonads.

A recent study showed that conditional knockout of *mTOR* in primordial follicles reversed granulosa cells into Sertoli-like cells, along with several testicular properties in ovary tissues [38]. Though involving alternate gonads, these two studies support each other and together establish the critical role of mTOR or its binding partner in maintaining supporting cell fate and gonad development and function. However, since mTOR is present in both mTORC1 and mTORC2, the deletion of mTOR should block both pathways. Thus it is unclear whether the ovary-to-testis reversal observed in that study was due to single inactivation of either mTORC1 or mTORC2, or both, yet this issue was not clearly addressed in that study. Our study provided evidence that blocking mTORC1 alone (by *Raptor* deletion) can induce an SC dedifferentiation and a subtle ovary-like reorganization.

Our previous study revealed that mutant mice with SC-specific inactivation of Rheb, a direct upstream activator of mTORC1, displayed almost normal tubular histomorphology and functions [35]. Thus, we deemed that Raptor may function independently of canonical Rheb/mTORC1 signaling to control postnatal SC differentiation and testis development. Evidence supporting this notion also came from another study demonstrating that mTORC1-independent ("free") Raptor negatively regulated hepatic Akt activity and lipogenesis [57], suggesting Raptor does not simply function as a scaffold in mTORC1. In addition, we previously showed that the ribosomal protein S6, a downstream target of canonical Rheb/mTORC1 signaling, was exclusively activated in differentiating spermatogonia but was scarcely detectable in SCs in postnatal testis [32], suggesting canonical mTORC1 signaling plays a limited role in postnatal SCs. Moreover, it is worthwhile to note that the International Mouse Phenotyping Consortium recently published a resource of targeted mutant mouse lines for 5061 genes [58], which reported that *mTOR* knockout mice showed preweaning lethality and died as early adults (ID: 1928394), whereas *Raptor* knockout mice exhibited embryonic lethality before tooth bud stage and died at E12.5 (ID: 1921620). This suggested that Raptor is more important than mTOR for embryo development and controls critical biological processes independently of mTOR. These observations support ascribing SC dedifferentiation and potential cell fate transition (SC to granulosa cell) in the *Raptor* mutant gonads to inactivating "free" Raptor rather than canonical mTORC1 signaling. Further study of conditional ablation of *mTOR* in SCs, or alternatively, *Raptor* in oocytes, will help define whether "free" Raptor exists and what role it plays in gonadal sex differentiation, identity maintenance, and gonad development.

As SC dedifferentiated, the size of adult *Raptor* mutant gonads was greatly decreased (Figure 1B), with an adult testis mass of only ~6% of the controls. This was not observed in the *Dmrt1* mutant testes or the *mTOR* or *Foxl2* mutant ovaries. We ascribed this specific phenotype mainly to *Raptor* deletion-reduced proliferation of three types of cells: (1) SCs. Besides maintaining SC identity, we believe that Raptor is also essential for the second intensive proliferation of SCs, which takes place in the first two weeks after birth in mice and is vital for the expansion and mature of testicular cords [59]. Indeed, Raptor was intensively expressed in mouse SCs across embryonic and postnatal periods (Supplemental Figure S5). (2) Male germ cells, all biochemical activities of which exclusively rely on SCs; evidence for this came from the observation obtained by excessive germ cell loss in histology and Ki67 staining showing insufficient germ cell proliferation. (3) Granulosa cells. Potentially transdifferentiated granulosa-like cells also likely required Raptor to support the expansion of their population, which is required for follicle growth and ovary development. In addition, increased apoptotic activity was probably a second cause of gonad shrinking, and perhaps altered gene expression activity was the effect of *Raptor* deletion (Figure 2C).

In summary, we established that Raptor is required for stabilizing postnatal SC characteristics and testicular architecture. Ablation of *Raptor* converted postnatal SCs into an undifferentiated state, and they presented some ovarian somatic cell-like features and can produce estrogen. Our study extends the current knowledge of maintenance of postnatal male somatic cell characteristics and testis development. Although we provided in vitro evidence suggesting Raptor is involved in FGF9 signaling in the regulation of SC maturation, an in vivo study is needed to unravel further whether Raptor acts downstream of FGF9 signaling or in parallel to stabilize the male route, dependently or independently of mTOR. This would greatly enrich our understanding of gonadal sex differentiation, maintenance, and gonad development and contribute to new ideas for the prevention and therapy for hermaphroditism or infertility.

Supplementary material

Supplementary material is available at *BIOLRE* online.

Data availability

RNA-seq data have been deposited in the NCBI SRA database (PRJNA767807). Other data are available upon reasonable request.

Funding

This work was supported by the National Natural Science Foundation of China [32171113, 31972910, 82071723, 81871162], Guangdong Basic and Applied Basic Research Foundation [2021A1515010774, 2021B1515020069, 2019A1515010755], Guangdong Medical Science and Technology Research Foundation [A2020080], The Science and Technology Project of Guangzhou [202002030063], The Health Science and Technology Project of Guangzhou [20201A011016, 201904010024], and The Scientific Program of Dongguan People's Hospital (K202022).

Conflict of interest

The authors declare no conflict of interest.

References

1. Gubbay J, Collignon J, Koopman P, Capel B, Economou A, Munsterberg A, Vivian N, Goodfellow P, Lovell-Badge R. A gene mapping to the sex-determining region of the mouse Y chromosome is a member of a novel family of embryonically expressed genes. *Nature* 1990; **346**:245–250.
2. Koopman P, Gubbay J, Vivian N, Goodfellow P, Lovell-Badge R. Male development of chromosomally female mice transgenic for Sry. *Nature* 1991; **351**:117–121.

3. Bullejos M, Koopman P. Spatially dynamic expression of Sry in mouse genital ridges. *Dev Dyn* 2001; **221**:201–205.
4. Hacker A, Capel B, Goodfellow P, Lovell-Badge R. Expression of Sry, the mouse sex determining gene. *Development* 1995; **121**: 1603–1614.
5. Sekido R, Bar I, Narvaez V, Penny G, Lovell-Badge R. SOX9 is up-regulated by the transient expression of SRY specifically in Sertoli cell precursors. *Dev Biol* 2004; **274**:271–279.
6. Wilhelm D, Hiramatsu R, Mizusaki H, Widjaja L, Combes AN, Kanai Y, Koopman P. SOX9 regulates prostaglandin D synthase gene transcription in vivo to ensure testis development. *J Biol Chem* 2007; **282**:10553–10560.
7. Malki S, Nef S, Notarnicola C, Thevenet L, Gasca S, Mejean C, Berta P, Poulat F, Boizet-Bonhoure B. Prostaglandin D2 induces nuclear import of the sex-determining factor SOX9 via its cAMP-PKA phosphorylation. *EMBO J* 2005; **24**:1798–1809.
8. Wilhelm D, Martinson F, Bradford S, Wilson MJ, Combes AN, Beverdam A, Bowles J, Mizusaki H, Koopman P. Sertoli cell differentiation is induced both cell-autonomously and through prostaglandin signaling during mammalian sex determination. *Dev Biol* 2005; **287**:111–124.
9. Kim Y, Kobayashi A, Sekido R, DiNapoli L, Brennan J, Chaboissier MC, Poulat F, Behringer RR, Lovell-Badge R, Capel B. Fgf9 and Wnt4 act as antagonistic signals to regulate mammalian sex determination. *PLoS Biol* 2006; **4**:e187.
10. Miyawaki S, Tachibana M. Role of epigenetic regulation in mammalian sex determination. *Curr Top Dev Biol* 2019; **134**:195–221.
11. Dupont S, Capel B. The chromatin state during gonadal sex determination. *Sex Dev* 2021; **15**:308–316.
12. Tomizuka K, Horikoshi K, Kitada R, Sugawara Y, Iba Y, Kojima A, Yoshitome A, Yamawaki K, Amagai M, Inoue A, Oshima T, Kakitani M. R-spondin1 plays an essential role in ovarian development through positively regulating Wnt-4 signaling. *Hum Mol Genet* 2008; **17**:1278–1291.
13. Chassot AA, Ranc F, Gregoire EP, Roepers-Gajadien HL, Taketo MM, Camerino G, de Rooij DG, Schedl A, Chaboissier MC. Activation of beta-catenin signaling by Rspo1 controls differentiation of the mammalian ovary. *Hum Mol Genet* 2008; **17**:1264–1277.
14. Chassot AA, Gillot I, Chaboissier MC. R-spondin1, WNT4, and the CTNNB1 signaling pathway: strict control over ovarian differentiation. *Reproduction* 2014; **148**:R97–R110.
15. Li Y, Zhang L, Hu Y, Chen M, Han F, Qin Y, Cui X, Duo S, Tang F, Gao F. Beta-catenin directs the transformation of testis Sertoli cells to ovarian granulosa-like cells by inducing Foxl2 expression. *J Biol Chem* 2017; **292**:17577–17586.
16. Ottolenghi C, Omari S, Garcia-Ortiz JE, Uda M, Crisponi L, Forabosco A, Pilia G, Schlessinger D. Foxl2 is required for commitment to ovary differentiation. *Hum Mol Genet* 2005; **14**:2053–2062.
17. Uhlenhaut NH, Jakob S, Anlag K, Eisenberger T, Sekido R, Kress J, Treier AC, Klugmann C, Klasen C, Holter NI, Riethmacher D, Schutz G *et al.* Somatic sex reprogramming of adult ovaries to testes by FOXL2 ablation. *Cell* 2009; **139**:1130–1142.
18. Yao HH, Matzuk MM, Jorgez CJ, Menke DB, Page DC, Swain A, Capel B. Follistatin operates downstream of Wnt4 in mammalian ovary organogenesis. *Dev Dyn* 2004; **230**:210–215.
19. Yao HH, Whoriskey W, Capel B. Desert hedgehog/patched 1 signaling specifies fetal Leydig cell fate in testis organogenesis. *Genes Dev* 2002; **16**:1433–1440.
20. Brennan J, Tilmann C, Capel B. Pdgfr-alpha mediates testis cord organization and fetal Leydig cell development in the XY gonad. *Genes Dev* 2003; **17**:800–810.
21. Gao F, Maiti S, Alam N, Zhang Z, Deng JM, Behringer RR, Lecureuil C, Guillou F, Huff V. The Wilms tumor gene, Wt1, is required for Sox9 expression and maintenance of tubular architecture in the developing testis. *Proc Natl Acad Sci U S A* 2006; **103**: 11987–11992.
22. Garcia-Moreno SA, Lin YT, Futtner CR, Salamone IM, Capel B, Maatouk DM. CBX2 is required to stabilize the testis pathway by repressing Wnt signaling. *PLoS Genet* 2019; **15**:e1007895.
23. Meeks JJ, Weiss J, Jameson JL. Dax1 is required for testis determination. *Nat Genet* 2003; **34**:32–33.
24. Swain A, Narvaez V, Burgoyne P, Camerino G, Lovell-Badge R. Dax1 antagonizes Sry action in mammalian sex determination. *Nature* 1998; **391**:761–767.
25. Bashamboo A, Eozenou C, Jorgensen A, Bignon-Topalovic J, Siffroi JP, Hyon C, Tar A, Nagy P, Solyom J, Halasz Z, Paye-Jaouen A, Lambert S *et al.* Loss of function of the nuclear receptor NR2F2, encoding COUP-TF2, causes testis development and cardiac defects in 46. *XX Children Am J Hum Genet* 2018; **102**: 487–493.
26. Nicol B, Grimm SA, Chalmel F, Lecluze E, Pannetier M, Pailhoux E, Dupin-De-Beyssat E, Guiguen Y, Capel B, Yao HH. RUNX1 maintains the identity of the fetal ovary through an interplay with FOXL2. *Nat Commun* 2019; **10**:5116.
27. Matson CK, Murphy MW, Sarver AL, Griswold MD, Bardwell VJ, Zarkower D. DMRT1 prevents female reprogramming in the postnatal mammalian testis. *Nature* 2011; **476**:101–104.
28. Bai X, Jiang Y. Key factors in mTOR regulation. *Cell Mol Life Sci* 2010; **67**:239–253.
29. Liu GY, Sabatini DM. mTOR at the nexus of nutrition, growth, ageing and disease. *Nat Rev Mol Cell Biol* 2020; **21**:183–203.
30. Wang Y, Zhang H. Regulation of autophagy by mTOR signaling pathway. *Adv Exp Med Biol* 2019; **1206**:67–83.
31. Ben-Sahra I, Manning BD. mTORC1 signaling and the metabolic control of cell growth. *Curr Opin Cell Biol* 2017; **45**:72–82.
32. Wang C, Wang Z, Xiong Z, Dai H, Zou Z, Jia C, Bai X, Chen Z. mTORC1 activation promotes spermatogonial differentiation and causes subfertility in mice. *Biol Reprod* 2016; **95**:97.
33. Hobbs RM, La HM, Makela JA, Kobayashi T, Noda T, Pandolfi PP. Distinct germline progenitor subsets defined through Tsc2-mTORC1 signaling. *EMBO Rep* 2015; **16**:467–480.
34. Dong H, Chen Z, Wang C, Xiong Z, Zhao W, Jia C, Lin J, Lin Y, Yuan W, Zhao AZ, Bai X. Rictor regulates spermatogenesis by controlling Sertoli cell cytoskeletal organization and cell polarity in the mouse testis. *Endocrinology* 2015; **156**:4244–4256.
35. Xiong Z, Wang C, Wang Z, Dai H, Song Q, Zou Z, Xiao B, Zhao AZ, Bai X, Chen Z. Raptor directs Sertoli cell cytoskeletal organization and polarity in the mouse testis. *Biol Reprod* 2018; **99**:1289–1302.
36. Mok KW, Mruk DD, Cheng CY. Regulation of blood-testis barrier (BTB) dynamics during spermatogenesis via the "Yin" and "Yang" effects of mammalian target of rapamycin complex 1 (mTORC1) and mTORC2. *Int Rev Cell Mol Biol* 2013; **301**:291–358.
37. Boyer A, Girard M, Thimmanahalli DS, Levasseur A, Celeste C, Paquet M, Duggavathi R, Boerboom D. mTOR regulates gap junction alpha-1 protein trafficking in Sertoli cells and is required for the maintenance of spermatogenesis in mice. *Biol Reprod* 2016; **95**:13.
38. Guo J, Zhang T, Guo Y, Sun T, Li H, Zhang X, Yin H, Cao G, Yin Y, Wang H, Shi L, Guo X *et al.* Oocyte stage-specific effects of MTOR determine granulosa cell fate and oocyte quality in mice. *Proc Natl Acad Sci U S A* 2018; **115**:E5326–E5333.
39. Nenicu A, Luers GH, Kovacs W, David M, Zimmer A, Bergmann M, Baumgart-Vogt E. Peroxisomes in human and mouse testis: differential expression of peroxisomal proteins in germ cells and distinct somatic cell types of the testis. *Biol Reprod* 2007; **77**: 1060–1072.
40. Chaboissier MC, Kobayashi A, Vidal VI, Lutzkendorf S, van de Kant HJ, Wegner M, de Rooij DG, Behringer RR, Schedl A. Functional analysis of Sox8 and Sox9 during sex determination in the mouse. *Development* 2004; **131**:1891–1901.
41. Mullen RD, Behringer RR. Molecular genetics of Mullerian duct formation, regression and differentiation. *Sex Dev* 2014; **8**: 281–296.
42. Cheng CY, Chen CL, Feng ZM, Marshall A, Bardin CW. Rat clusterin isolated from primary Sertoli cell-enriched culture medium is sulfated glycoprotein-2 (SGP-2). *Biochem Biophys Res Commun* 1988; **155**:398–404.

43. Yomogida K, Ohtani H, Harigae H, Ito E, Nishimune Y, Engel JD, Yamamoto M. Developmental stage- and spermatogenic cycle-specific expression of transcription factor GATA-1 in mouse Sertoli cells. *Development* 1994; **120**:1759–1766.
44. Mendis SH, Meachem SJ, Sarraj MA, Loveland KL. Activin a balances Sertoli and germ cell proliferation in the fetal mouse testis. *Biol Reprod* 2011; **84**:379–391.
45. Rebourcet D, Mackay R, Darbey A, Curley MK, Jorgensen A, Frederiksen H, Mitchell RT, O'Shaughnessy PJ, Nef S, Smith LB. Ablation of the canonical testosterone production pathway via knockout of the steroidogenic enzyme HSD17B3, reveals a novel mechanism of testicular testosterone production. *FASEB J* 2020; **34**:10373–10386.
46. Hogarth CA, Evans E, Onken J, Kent T, Mitchell D, Petkovich M, Griswold MD. CYP26 enzymes are necessary within the postnatal seminiferous epithelium for normal murine spermatogenesis. *Biol Reprod* 2015; **93**:19.
47. Birk OS, Casiano DE, Wassif CA, Cogliati T, Zhao L, Zhao Y, Grinberg A, Huang S, Kreidberg JA, Parker KL, Porter FD, Westphal H. The LIM homeobox gene Lhx9 is essential for mouse gonad formation. *Nature* 2000; **403**:909–913.
48. Couse JF, Hewitt SC, Bunch DO, Sar M, Walker VR, Davis BJ, Korach KS. Postnatal sex reversal of the ovaries in mice lacking estrogen receptors alpha and beta. *Science* 1999; **286**: 2328–2331.
49. Tsuchiya Y, Nakajima M, Yokoi T. Cytochrome P450-mediated metabolism of estrogens and its regulation in human. *Cancer Lett* 2005; **227**:115–124.
50. Stevant I, Kuhne F, Greenfield A, Chaboissier MC, Dermitzakis ET, Nef S. Dissecting cell lineage specification and sex fate determination in gonadal somatic cells using single-cell transcriptomics. *Cell Rep* 2019; **26**:3272, e3273–3283.
51. Mazaud S, Oreal E, Guigon CJ, Carre-Eusebe D, Magre S. Lhx9 expression during gonadal morphogenesis as related to the state of cell differentiation. *Gene Expr Patterns* 2002; **2**:373–377.
52. Lin YT, Barske L, DeFalco T, Capel B. Numb regulates somatic cell lineage commitment during early gonadogenesis in mice. *Development* 2017; **144**:1607–1618.
53. Haider SG. Cell biology of Leydig cells in the testis. *Int Rev Cytol* 2004; **233**:181–241.
54. Skinner MK. Regulation of primordial follicle assembly and development. *Hum Reprod Update* 2005; **11**:461–471.
55. Okeigwe I, Kuohung W. 5-alpha reductase deficiency: a 40-year retrospective review. *Curr Opin Endocrinol Diabetes Obes* 2014; **21**:483–487.
56. Schmahl J, Kim Y, Colvin JS, Ornitz DM, Capel B. Fgf9 induces proliferation and nuclear localization of FGFR2 in Sertoli precursors during male sex determination. *Development* 2004; **131**: 3627–3636.
57. Kim K, Qiang L, Hayden MS, Sparling DP, Purcell NH, Pajvani UB. mTORC1-independent raptor prevents hepatic steatosis by stabilizing PHLPP2. *Nat Commun* 2016; **7**:10255.
58. Birling MC, Yoshiki A, Adams DJ, Ayabe S, Beaudet AL, Bottomley J, Bradley A, Brown SDM, Burger A, Bushell W, Chiani F, Chin HG *et al.* A resource of targeted mutant mouse lines for 5,061 genes. *Nat Genet* 2021; **53**:416–419.
59. Sharpe RM, McKinnell C, Kivlin C, Fisher JS. Proliferation and functional maturation of Sertoli cells, and their relevance to disorders of testis function in adulthood. *Reproduction* 2003; **125**: 769–784.